Volume 14, Issue 3, 142428 (1-14)

Iranian Journal of Catalysis (IJC)

https://doi.org/10.57647/j.ijc.2024.1403.28

Magnetite-supported salicylic acid (Fe_3O_4@SA) as a magnetically separable and reusable catalyst for the synthesis of 3, 4 dihydropyrimidin-2(1H)-ones/thiones and benzylidenemalononitrile derivatives under solvent-free conditions

Dhananjay N. Gaikwad[1], Suresh T. Gaikwad*[2], Rajesh K. Manjul[2], Dayanand M. Suryavanshi[3], Anjali S. Rajbhoj[2], Swapnil R. Bankar[4], Santosh T. Shinde[5], Nilam S. Dhane[1]

[1]*Department of Chemistry, Yashavantrao Chavan Institute of Science, Satara, Maharashtra, India.*
[2]*Department of Chemistry, Dr. Babasaheb Ambedkar Marathwada University, Aurangabad, Maharashtra, India.*
[3]*P. G. and Research department Of Chemistry, S. S. G. M., College, Kopargaon, Dist. A. Nagar, Maharashtra, India.*
[4]*Dept.of. Chemistry, Sharadchandra Pawar Mahavidyalay, Lonand, Dist. Satara, Maharashtra, India.*
[5]*P. G. department Of Chemistry, Annasaheb Awate College, Manchar, Dist. Pune, Maharashtra, India.*

*Corresponding authors: gaikwadsuresh12@gmail.com

Original Research

Received:
25 March 2024
Revised:
14 June 2024
Accepted:
2 July 2024
Published online:
10 July 2024

Abstract:

The use of the new Fe_3O_4@Salicylic acid nanocatalyst (Fe_3O_4@SA) is described in the synthesis of 3, 4 dihydropyrimidin-2(1H)-ones/thiones and benzylidenemalononitrile in a solvent-free (SF) environment at 80°C as a simple, effective, and environmentally friendly procedure. In the present protocol, we have created new, simple chemical co-precipitation method for the synthesis of efficient and magnetically recoverable Fe_3O_4 magnetic nanoparticles (MNPs) coated with a layer of salicylic acid. The synthesized catalyst underwent thorough characterization successfully by Infrared spectroscopy, Powder X-ray diffraction (XRD), Field emission scanning electron microscopy (FESEM), Transmission electron microscopy (TEM), and FESEM-energy-dispersive X-ray spectroscopy, Thermogravimetric analysis (TGA), Vibrating sample magnetometer (VSM) respectively. This eco-friendly and green synthesis methodology has advantages, such as the absence of hazardous organic solvents, magnetic in nature, salicylic acid coated ferrite nanocatalysts are easily separable and reusable, quick reaction time and large product yield(71-98%), making this protocol superior and robust.

Keywords: Nanocatalyst; Biginelli; Dihydropyrimidine; Green synthesis; Multicomponent reaction; Solvent-free Fe_3O_4; One-pot synthesis

1. Introduction

Nanocatalyst research has always been one of the most fascinating areas of study in green chemistry and nanochemistry. Over the past ten years, researchers have carried out a great deal of study on nanocatalysts. By bridging the gap between homogeneous and heterogeneous catalysts, nanocatalysts can take advantage of both. In order to separate and recover from the reaction mixture, chemists have tried to develop high-activity and high-efficiency catalysts with

good selectivity, low energy consumption, and extended life [1–3]. Magnetic nanoparticles are used in a variety of fields, including environmental remediation, biotechnology, biomedicine, and catalysis [4]. They also offer a number of benefits, including strong catalytic activity, reusability, chemical stability in a range of organic solvents, and simplicity of separation with the use of an external magnet [5, 6]. These nanocatalyst's magnetic properties have resulted in their facile separation and recovery from the reaction system [7]. Furthermore, magnetic nanoparticles have garnered significant interest among researchers in recent years, and iron nanoparticles are particularly important among magnetic nanoparticles [8]. Nontoxic Lewis acids such as iron nanoparticles (ions) have been used as catalysts in many cases [9, 10]. Applications for magnetic iron nanoparticles are not restricted to a single field but include a wide range of fields, for instance, magnetic hyperthermia [11, 12], culinary science [13], imaging using magnetic resonance (MRI) [14], fluid transfer, microbiology, and drug delivery [15–19]. Multidisciplinary materials heavily rely on functionalized magnetic metal nanoparticles. Numerous other academic and professional domains, including chemistry, biology, pharmacology, optics, electronics, catalyst sciences, and technologies [20].

Using urea or thiourea, aromatic aldehydes, b-dicarbonyl compounds, and Fe_3O_4 in one-pot Biginelli reactions, an appealing class of dihydropyrimidinone derivatives were synthesized with high to exceptional yield [21]. For instance, many acid coated magnetic particles, as well as their application in the synthesis of heterocyclic compounds, were investigated in Bigineli reactions such as nanoparticles of phosphomolybdic acid on imidazole-functionalized Fe_3O_4@SiO_2 [22], Fe_3O_4-DOPA-Cu [23], isoniazid-functionalized Fe_3O_4 (Fe_3O_4@SiO_2-Pr-INH) [24], Fe_3O_4-MWCNT [25], Fe_3O_4@silica sulfuric acid [26], sulfamic acid supported magnetic Fe_3O_4 [27], mercaptopropanoic acid coated Fe_3O_4 [28], sulfonated-phenylacetic acid coated Fe_3O_4 [29], PTA@ZIF- 9(NH_2)[30] etc. The synthesis of bioactive chemicals has shown considerable interest in multicomponent reactions [31–33]. The cyclocondensation of aldehydes, suitable C-H acidic carbonyl compounds, and urea-type building blocks under acidic conditions provides multifunctionalised dihydropyrimidine derivatives [34]. The biological investigation of these various molecules via molecular manipulation showed activities such as antihypertensive drugs, calcium channel blockers, a-1a antagonists, possible TLR4 antagonists, antiviral, antitumor, anti-inflammatory, antibacterial, antifungal, and antitubercular activity[35–48].

In organic chemistry, derivatives of benzylidenemalononitrile (BMN) are widely employed as target and intermediate molecules. Benzylidenemalononitrile compound's special qualities, namely their antifungal [49], anticancer [50], antimicrobial [51], and anti-corrosive capabilities [52], have drawn the interest of numerous experts.

BMN compounds are employed in prostaglandin production, photoconductive cell design, oxidative stress cell resistance, and the inhibition or activation of specific enzymes [53]. In literature, many catalysts such as Fe_3O_4@SiO_2 [54], MgO/ZrO_2 [55], MIL-53(Fe) @SiO_2@$NiFe_2O_4$ [56], Fe_3O_4–cysteamine [57], Fe_3O_4@GO@PAMAM (G2) [58], Fe_3O_4@SiO_2@PAMAM-G_2 [59] etc., have been employed in the synthesis of BMN.

Because organic solvents are toxic, researchers are increasingly interested in organic reactions in solvent-free media. In the absence of solvents, the desired products were obtained with high yields within relatively brief reaction periods [60]. In a green manner, the procedure is not only environmentally friendly, but it also has a higher rate, higher yields, and takes less time. This protocol is both economical and environmentally friendly for organic synthesis. Furthermore, our approach supports the practical application of Fe_3O_4@SA nanocomposites as catalysts.

Here, we created a very effective functional magnetic acid catalyst by examining the impact of immobilizing salicylic acids -OH and -COOH groups on Fe_3O_4 nanomagnetic particles as a substrate. In order to synthesize 3, 4-dihydropyrimidine-2(1H)-ones/thiones and benzylidenemalononitrile (BMN) under mild circumstances, this article has attempted to present a useful and practical approach for the Biginelli and Knoevenagel condensation processes, respectively.

2. Experimental

2.1 Materials and reagents

All chemicals were procured from Avra Lab. and utilized without additional purification. The reaction's progression was tracked through thin-layer chromatography (TLC), employing Merck's analytical and preparative thin-layer chromatography plates with 0.2 mm and 0.5 mm Kieselgel GF 254 pre-coated aluminium plates, respectively. UV light chambers were utilized for visualizing the spots. Proton (^{1}H) and carbon (^{13}C) nuclear magnetic resonance (NMR) spectra were acquired on a Bruker Avance 500 MHz spectrometer using DMSO-d_6 and $CDCl_3$ as solvents, with tetramethylsilane (TMS) serving as an internal reference standard. Chemical shifts are reported in δ (parts per million). Infrared (IR) spectra were obtained using a Perkin Elmer spectrophotometer with potassium bromide (KBR) discs. The particle morphology, size, elemental composition, thermal stability, and magnetic property of the synthesized catalyst nanomaterial were characterized using a Field Emission Scanning Electron Microscope (FESEM) - Hitachi High-Tech SU8000, and Single Crystal-X-Ray Diffractometer (SC-XRD) - Bruker (D8 Venture). Energy-dispersive X-ray spectroscopy (EDS) analysis was conducted using FESEM, TGA- Hitachi NEXTA STA300, and MICROSENSE EZ-9, respectively.

2.2 Synthesis of Fe_3O_4@salicylic acid catalyst

Iron sulfate heptahydrate ($FeSO_4.7H_2O$) 2.78 g and ferric chloride ($FeCl_3$) 3.24 g were combined with a molar ratio of 1:2, with 10 mL of each solution added. A sodium hydroxide (NaOH) solution was prepared by dissolving 14.4 g (1.8 mol) of NaOH solid in 200 mL of distilled water and preheating it to approximately 80 °C. The mixed solution of $FeSO_4.7H_2O$ and $FeCl_3$ was then added dropwise to the preheated NaOH solution under continuous stirring,

maintaining the temperature at 80 °C for 15 minutes. The resulting reaction mixture was stirred for an additional 15 minutes, yielding a black precipitate consisting of iron oxide nanoparticles. Subsequently, a coating agent comprising 12 wt. % (0.227 g) salicylic acid was added dropwise to the solution under vigorous stirring at 90 °C for 1 hour. Once the stirring stopped, the solution was subjected to sonication for 2 hours. Upon cooling, the precipitate settled at the bottom and was filtered using whatman No. 42 filter paper. The obtained precipitate was washed several times with aqueous alcohol to remove impurities, followed by drying of the catalyst in an oven at 100 °C.

2.3 Synthesis of 3, 4 dihydropyrimidin-2(1H)-ones/ thiones by using Fe_3O_4@SA nanocatalyst

The mixture of **1a**:0.106 g; **1b**:0.140 g; **1c**:0.124 g; **1d**: 0.122 g, **1e**:0.151 g, **1f**:0.166 g (1 mmol) of aromatic aldehyde, 0.130 g (1 mmol) of ethyl acetoacetate, 0.072 g /0.091 g (1.2 mmol) of urea/thiourea and 0.050 g of Fe_3O_4@SA magnetic nanoparticles in round bottom flask was stirred at 80 °C in oil bath on magnetic stirrer without the use of solvents. After TLC, the reaction mixture was allowed to cool to room temperature using an eluent ratio of petroleum ether to ethyl acetate of 8:2. The resultant solid was dissolved in ethyl acetate, and an external magnet was used to aid in separating the magnetic nanocatalyst. On a rota evaporator, the mixture was concentrated under low pressure. The resulting solid was then water-washed and recrystallized from ethanol.

2.4 Synthesiss of benzylidenemalononitrile by using Fe_3O_4@SA nanocatalyst

4a:0.184 g; **4b**:0.197 g; **4c**:0.362; **4d**: 0.310 g; **4e**:0.296 g (1 mmol) of the aldehyde derivative was combined with (1 mmol) 0.66 g of malononitrile in a reaction vessel. 0.050 g Fe_3O_4@SA catalyst was added, and the mixture underwent stirring in an oil bath at 80 °C under solvent free condition for 10-15 minutes. The resulting solid was dissolved using ethyl acetate, and using an external magnet, the magnetic nanoparticle catalyst was separated.The weight of the crude product was measured, and subsequently, its percentage yield and melting point were determined.

2.4.1 Spectral data of as-synthesized compounds

2.4.1.1 Ethyl 6-methyl-4-phenyl-2-thioxo-1, 2, 3, 4-tetrahydropyrimidine5-carboxylate (2a)

(Table 4, entry 1): ^{1}H NMR (DMSO-d_6, 500 MHz): δ 10.58 (1H, NH), 9.91 (1H, NH), 7.40-7.50 (m, 5H, H-2', H-3', H-4, H-5'& H- 6'), 5.42 (s, 1H, H-4), 4.22 (q, J = 7.1 Hz, 2H, $\underline{CH_2}$-CH_3), 2.41 (s, 3H, CH_3), 1.32 (t, J = 7.1 Hz, 3H, CH_2-$\underline{CH_3}$).

2.4.1.2 Ethyl4-(4-chlorophenyl)-6-methyl-2-thioxo-1,2,3,4-tetrahydropyrimidine 5carboxylate (2b)

Table 4, entry 2): ^{1}H NMR (DMSO-d_6, 500 MHz): δ 10.61 (s, 1H, NH), 9.96 (s, 1H, NH), 7.71 (d, J = 8.0 Hz, 2H, H-3'& H-5'), 7.52 (d, J = 8.0 Hz, 2H, H-2' & H-6'), 5.41 (s, 1H, H-4), 4.24 (q, J = 7.1 Hz, 2H, $\underline{CH_2}$-CH_3), 2.82 (s, 3H, CH_3), 1.25 (t, J = 7.1 Hz, 3H, CH_2-$\underline{CH_3}$).

2.4.1.3 Ethyl4-(4-fluorophenyl)-6-methyl-2-thioxo-1, 2, 3, 4-tetrahydropyrimidine-5 carboxylate (2c)

(Table 4, entry 3): ^{1}H NMR (DMSO-d_6, 500 MHz) : δ 10.61 (s, 1H, NH), 9.91 (s, 1H, NH), 7.42 (m, 4H, H-2', H-3', H-5' & H-6'), 5.22 (s, 1H, H-4), 4.22 (q, J = 7.1 Hz, 2H, $\underline{CH_2}$-CH_3), 2.54 (s, 3H, CH_3), 1.24 (t, J = 7.1 Hz, 3H, CH_2-$\underline{CH_3}$).

2.4.1.4 Ethyl 4-(4-hydroxyphenyl)-6-methyl-2-thioxo -1, 2, 3, 4 tetrahydropyrimidine-5-carboxylate (2d)

(Table 4, entry 4): ^{1}H NMR (DMSO-d_6, 500 MHz): δ 9.12 (s, 1H, NH), 9.00 (s, 1H, NH), 7.52 (br s, 1H, OH), 7.21 (d, J = 7.91 Hz, 2H, H-2' & H-6'), 6.76 (d, J = 7.9 Hz, 2H, H-3' & H-5'), 5.22 (s, 1H, H-4), 4.12 (q, J = 6.7 Hz, 2H, $\underline{CH_2}$-CH_3), 2.32 (s, 3H, CH_3), 1.12 (t, J = 6.7 Hz, 3H, CH_2-$\underline{CH_3}$).

2.4.1.5 Ethyl 6-methyl-4-(4-nitrophenyl)-2-oxo-1, 2, 3, 4-tetrahydropyrimidine-5-carboxylate (2e)

(Table 4, entry 5): ^{1}H NMR (DMSO-d_6, 500 MHz): δ 9.36 (bs, 1H,NH), 8.17 (d, J = 7.6 Hz, 2H, H-3'& H-5'), 7.88 (bs, 1H, NH), 7.47 (d, J = 7.60 Hz, 2H, H-2', & H-6'), 5.42 (s, 1H, H-4), 3.97 (q, J = 7.1 Hz, 2H, $\underline{CH_2}$-CH_3), 2.47 (s, 3H, CH_3), 1.08 (t, J = 7.1 Hz, 3H, CH_2-$\underline{CH_3}$).

2.4.1.6 Ethyl 4-(3, 4-dimethoxyphenyl)-6-methyl-2-oxo-1, 2, 3, 4- tetrahydropyrimidine-5-carboxylate (2f)

(Table 4, entry 6): ^{1}H NMR ($CDCl_3$, 500 MHz): δ 8.40 (s,1H, NH), 7.24 (d, J = 8 Hz, 2H, H-5' & H-6'), 6.79(s, 1H, H-2'), 5.93 (s, 1H, NH), 5.35 (s, 1H, H-4), 4.04 (q, J = 8.0 Hz, 2H, CH_2-CH_3), 2.30(s, 3H, CH_3), 1.17 (t, J = 8.0 Hz, 3H, CH_2-$\underline{CH_3}$).

2.4.1.7 Ethyl 6-methyl-2-oxo-4-phenyl-1, 2, 3, 4-tetrahydro- pyrimidine-5-carboxylate (2g)

(Table 4, entry 7): ^{1}H NMR (DMSO-d_6, 500 MHz): δ 9.26 (s, 1H, NH), 7.79(s, 1H, NH), 7.32 (m, 5H, H-2', H-3', H-4', H-5'& H-6'), 5.11(d, J = 3.4 Hz, 1H, H-4), 4.00 (q, J = 6.7 Hz, 2H, $\underline{CH_2}$-CH_3), 2.31 (s, 3H, CH_3), 1.10 (t, J = 6.7 Hz, 3H, CH_2-$\underline{CH_3}$).

2.4.1.8 Ethyl 4-(4-chlorophenyl)-6-methyl-2-oxo-1, 2, 3, 4- tetrahydropyrimidine-5-carboxylate (2h)

(Table 4, entry 8): ^{1}H NMR ($CDCl_3$, 500 MHz): δ 9.35 (s, 1H, NH), 7.27∼ 7.83 (m, 4H, H-2', H-3', H-5'& H-6'), 5.20 (s, 1H, NH), 5.41 (d, J = 4.0 Hz, 1H, H-4), 4.11 (q, J =8.0 Hz, 2H, CH_2-CH_3), 2.38 (s, 3H,CH_3), 1.22 (t, J = 8.0 Hz, 3H, CH_2-$\underline{CH_3}$).

2.4.1.9 Ethyl (4-fluorophenyl)-6-methyl-2-oxo-1, 2, 3, 4-tetrahydropyrimidine-5-carboxylate (2i)

(Table 4, entry 9): ^{1}H NMR ($CDCl_3$, 500 MHz) : δ 9.20 (s, 1H, NH), 7.79 (t, J = 8.0 Hz & 4.0 Hz 2H, H-2' & H-6'), 7.25(t, J = 12 Hz & 8.0 Hz 2H, H-3' & H-5'), 7.20 (s, 1H, NH), 5.19 (s, 1H, H-4), 3.96 (q, J = 7.1 Hz, 2H, $\underline{CH_2}$-CH_3), 2.26 (s, 3H, CH_3), 1.08 (t, J= 7.1 Hz, 3H, CH -$\underline{CH}$).

2.4.1.10 Ethyl 4-(4-hydroxyphenyl)-6-methyl-2-oxo-1, 2, 3, 4- tetrahydropyrimidine-5-carboxylate (2j)

(Table 4, entry 10): ^{1}H NMR (DMSO-d_6, 500 MHz): δ 8.61 (br s, 1H, NH), 7.14(d, J = 8Hz, 2H, H-2' & 6-H'), 6.80 (d, J = 8Hz 2H, H-3' & H-5'), 6.62 (s, 1H, NH) 5.12 (s, 1H, H-4), 4.21 (br s, 1H, OH), 4.03 (q, J = 7.2 Hz, 2H, $\underline{CH_2}$-CH_3), 2.21 (s, 3H, CH_3), 1.11 (t, J = 7.2 Hz, 3H, CH_2-$\underline{CH_3}$).

2.4.1.11 2-(4-methoxybenzylidene) malononitrile (4a)

(Table 5, entry 11) : ^{1}H-NMR (500MHz, $CDCl_3$): δ (ppm):7.98 (d, J = 8.8 Hz, 2H), 8.38 (s, 1H), 7.19 (d, J =

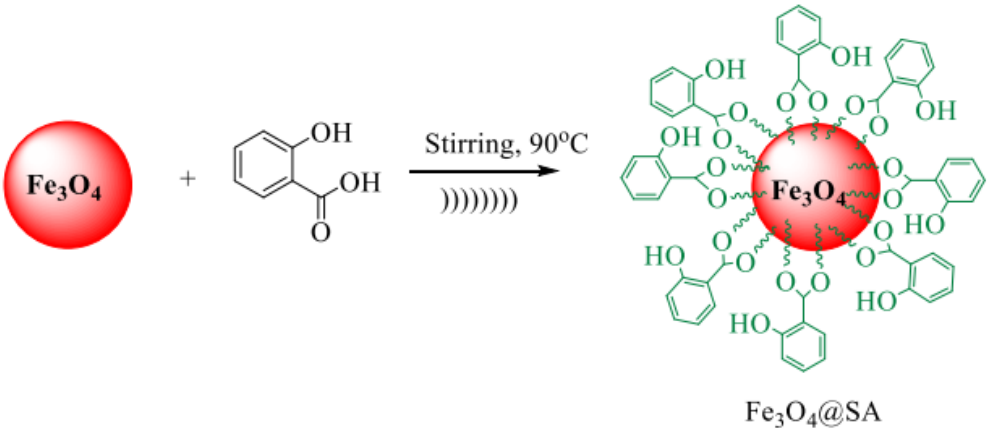

Scheme 1. Schematic representation of the synthesis of Fe_3O_4@SA nanocatalyst.

8.8 Hz, 2H), 3.89 (s, 3H); ^{13}C-NMR (500 MHz, $CDCl_3$) δ (ppm): 158.9, 154.4, 136.4, 128.9, 121.2, 120.2, 114.3, 112.9, 111.5, 81.5, 55.9.

2.4.1.12 2-(4-di methyl aminobenzylidene) malononitrile (4b)

(Table 5, entry 12): ^{1}H-NMR (500MHz, $CDCl_3$): δ 3.14 (s, 6H), 6.68 (d, 2H, J 9.3 Hz), 7.43 (s, 1H), 7.79 (d, 2H, J 9.3 Hz); ^{13}C-NMR (500 MHz, $CDCl_3$) δ (ppm): 40.02, 71.72, 111.54, 114.87, 115.94, 119.21, 133.72, 154.20, 157.98.

2.4.1.13 2-((3-(4-methoxyphenyl)-1-phenyl-1H-pyrazol-4-yl) methylene) malononitrile (4c)

(Table 5, entry 13): ^{1}H NMR (500 MHz, $CDCl_3$, δ, ppm): 3.88 (3H, s, O-CH_3), 7.05-7.81 (10H, m, HAr), 9.01 (1H, s, -CH=C $(CN)_2$). ^{13}C NMR (500 MHz, $CDCl_3$): 160.98, 156.24, 151.27, 138.63, 130.51, 129.81, 129.21, 128.58, 122.49, 120.07, 114.97, 114.72, 114.02, 113.94, 55.48

2.4.1.14 2-((1-phenyl-3-p-tolyl-1H-pyrazol-4-yl) methylene) malononitrile (4d)

(Table 5, entry 14): ^{1}H NMR (500 MHz, $CDCl_3$, δ, ppm): 2.44 (3H, s, -CH_3), 7.27-7.81 (10H, m, HAr), 9.02 (1H, s, -CH=C $(CN)_2$).^{13}C NMR (500 MHz, $CDCl_3$): 156.48, 151.25, 140.05, 138.63, 129.90, 129.80, 129.07, 129.22, 128.59, 127.24, 120.07, 115.02, 113.97, 113.92, 21.39.

3. Results and discussion

The process employed to construct the potent and magnetically recoverable catalyst Fe_3O_4@SA, which we synthesized in this work, is schematically depicted in Scheme 1. For the preparation of Fe_3O_4@SA nanocatalyst, we have developed a new method other than which was previously described by Unal et. al. in their research work.

The synthesized Fe_3O_4@SA was described, and its performance as a catalyst to produce dihydropyrimidinones was assessed in the Biginelli reaction. At a temperature of 80°C, the research entailed examining the Biginelli reaction model using urea, ethyl acetoacetate, and benzaldehyde as substrates (Scheme 2).

To maximize the reaction conditions and yield the highest catalytic activity, this process was conducted with different reaction parameters, including solvent and catalyst amount. The model reaction was carried out in a range of solvents as well as solvent-free conditions to assess the catalyst's efficacy (Table 1). As can be observed, the reaction produced the maximum yield (51%), even though it was conducted without the use of a solvent. Furthermore, various catalyst quantities were used to examine the influence of catalyst amount on the Biginelli reaction (Table 1). The product yield rose dramatically from 54% to 97% even though the amount of catalyst increased from 0.025 to 0.055 g. This is probably because there were more acid sites accessible. Since then, the yield percentage has stayed consistent between 0.050 and 0.055 g (Table 1, entries 1-10). The catalyst exhibits an average turnover number (TON) of 6860 mol and a turnover frequency (TOF) of 335 min^{-1}, both of

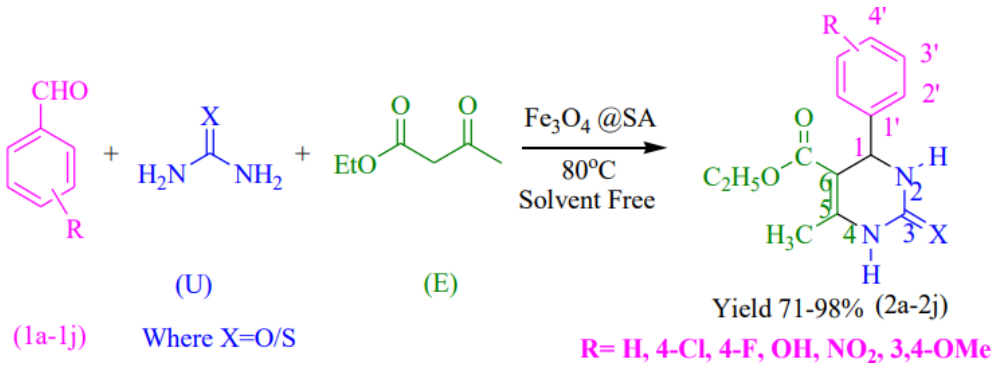

Scheme 2. Fe_3O_4@Salicylic acid catalyzed solvent-free one-pot synthesis of 3, 4 dihydropyrimidin-2(1H)-ones/thiones.

Table 1. The Biginelli reaction in the presence of Fe_3O_4@SA is affected by varying solvent concentrations and catalyst amounts.

Entry	Solvent	Catalyst (g)	Yield (%)
1	Water	(0.025)	Trace
2	Toluene	(0.025)	Trace
3	Ethanol	(0.025)	37
4	Acetonitrile	(0.025)	41
5	Solvent -free	No Catalyst	Trace
6	Solvent-free	(0.025)	51
7	Solvent-free	0.035	70
8	Solvent-free	0.040	87
9	Solvent-free	0.050	97
10	Solvent-free	0.055	97

Reaction condition: benzaldehyde (**1a**) (1 mmol, 0.106 g), ethyl acetoacetate **(E)**(1 mmol, 0.130 g), urea **(U)** (1.2 mmol, 0.072 g), catalyst(0.025-0.055 g), reaction time 60 min, reaction temperature 80 °C.

which demonstrate the catalyst's favorable efficiency.

We examined the viability of the reaction without a catalyst before utilizing it for a solvent-free reaction and discovered a trace amount of product. This demonstrates unequivocally that catalysts are needed for this process.

The catalyst's capacity to be reused is essential for industrial applications. To verify the catalyst's reusability in the model reaction, the reaction was run multiple times using the same batch of catalyst. Under optimal circumstances for the synthesis of the model compound 1a, as shown in Fig. 1, the catalyst's recyclability was investigated. Four times through the recycling process, no discernible decrease in activity was found. The four cycle's yields were noted as follows: 95%, 95%, 93%, and 90%, in that order. The catalyst was repeatedly washed in ethanol and magnetically separated after each cycle and deionized water to regenerate it. It was then utilized in the Biginelli reaction after being dried in a 60 °C oven.

Additionally, a comparison of the solvent and solvent-free catalytic activity of a few heterogeneous catalysts employed in Biginelli condensation was made. Fe_3O_4@SA was introduced as one of the most efficient heterogeneous catalysts for Biginelli condensation in a solvent-free environment. According to data, this Fe_3O_4@SA magnetic nano-catalyst formed the intended products quite efficiently when used under mild conditions and for a brief length of time (Table 2, entry 1-11).

Biginelli reactions of several aldehydes with urea (or thiourea) and ethyl acetoacetate were studied using Fe_3O_4@SA as the catalyst. The appropriate 3, 4-dihydropyrimidin-2(1H)-ones/thiones were produced in good to exceptional yields by the three-component reaction, which ran smoothly in all cases. Purity and high yields of the intended products were obtained through the reaction with aromatic aldehydes bearing electron-donating or electron-withdrawing groups. For Biginelli products, thiourea also offered acceptable yields (Table 3, entry 1-10).

Fig. 2 shows a probable mechanism for the synthesis of 3,

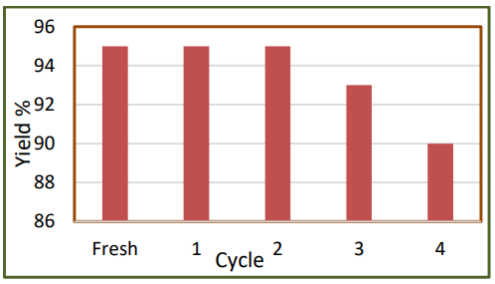

Figure 1. Recyclability of the catalyst.

Table 2. Catalytic activities of different catalysts for the synthesis of 3, 4-dihydropyrimidinone.

Entry	Catalyst	Temp (°C)	Time(min)	Yield (%)	Solvent	Ref.
1	Fe_3O_4@silica sulfuric acid	60	90	94	Solvent free	[30]
2	Sulfamic acid supported magnetic Fe_3O_4	100	60	89	Solvent free	[31]
3	Mercaptopropanoic acid coated Fe_3O_4	RT	120	95	Solvent free	[32]
4	Sulfonated-phenylacetic acid coated Fe_3O_4	RT	120	90	Solvent free	[33]
5	Phetalimid-N-sulfonic acid	120	120	94	Solvent free	[39]
6	Fe(III)/bentonite	80	420	95	Acetonitrile	[40]
7	Fe_3O_4@mesoporous SBA-15	90	360	85	Ethanol	[19]
8	Fe_3O_4@Nb_2O_5	80	720	99	Ethanol	[41]
9	PFAMPS	Reflux	300	87	Ethanol	[42]
10	*p*-Sulfonic acid calixarenes	Reflux	480	69	Ethanol	[43]
11	Fe_3O_4@SA	80	60	95	Solvent free	This work

The synthesis of 3, 4-dihydropyrimidinone is achieved by Biginelli condensation of urea **(U)**, ethyl acetoacetate **(E)**, and benzaldehyde **(1a)**. The catalytic act of certain heterogeneous solid acid catalysts is compared in solvent and solvent-free conditions.

Table 3. Synthesis of 3, 4-dihydropyrimidin-2(1H)-ones/thiones (2a-2j) by Fe_3O_4@SA catalyst at solvent-free condition (Scheme 2).

Entry	Sr. No.	Reactant	X= O/S	Time (min)	Product	[a]Yield %	M.P.
1	**2a**	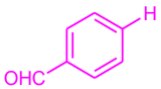	S	60	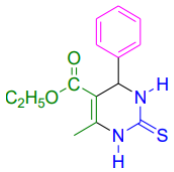	95	206 °C
2	**2b**	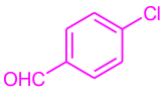	S	60	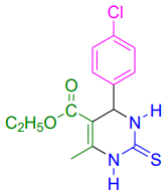	98	191 °C
3	**2c**	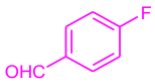	S	60	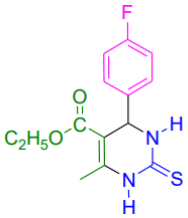	96	182 °C
4	**2d**	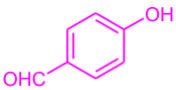	S	60	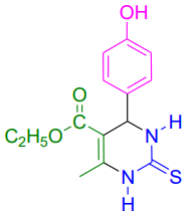	95	202 °C
5	**2e**	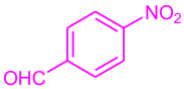	O	60	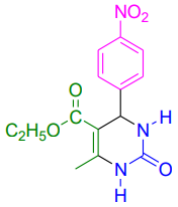	86	203 °C
6	**2f**	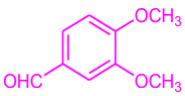	O	60	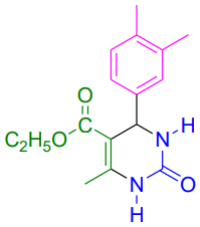	93	175 °C
7	**2g**	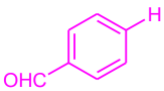	O	60	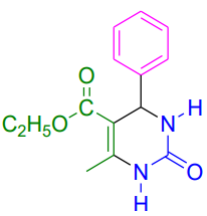	97	203 °C

Continue of Table 3.

Entry	Sr. No.	Reactant	X= O/S	Time (min)	Product	[a]Yield %	M.P.
8	**2h**	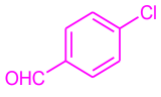	O	60	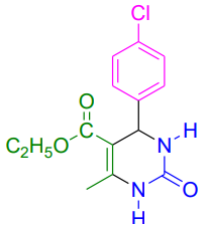	88	217 °C
9	**2i**	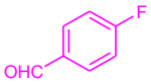	O	60	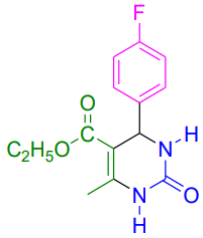	96	184 °C
10	**2j**	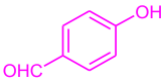	O	60	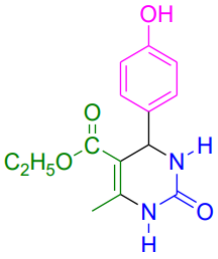	71	245 °C

Reaction condition: aromatic aldehyde (1 mmol), ethyl acetoacetate (1 mmol, 0.130 g), urea/thiourea (1.2 mmol, 0.072 g/ 0.091 g), catalyst (0.050 g), reaction time 60 min, reaction temperature 80 °C. [a] isolated yield.

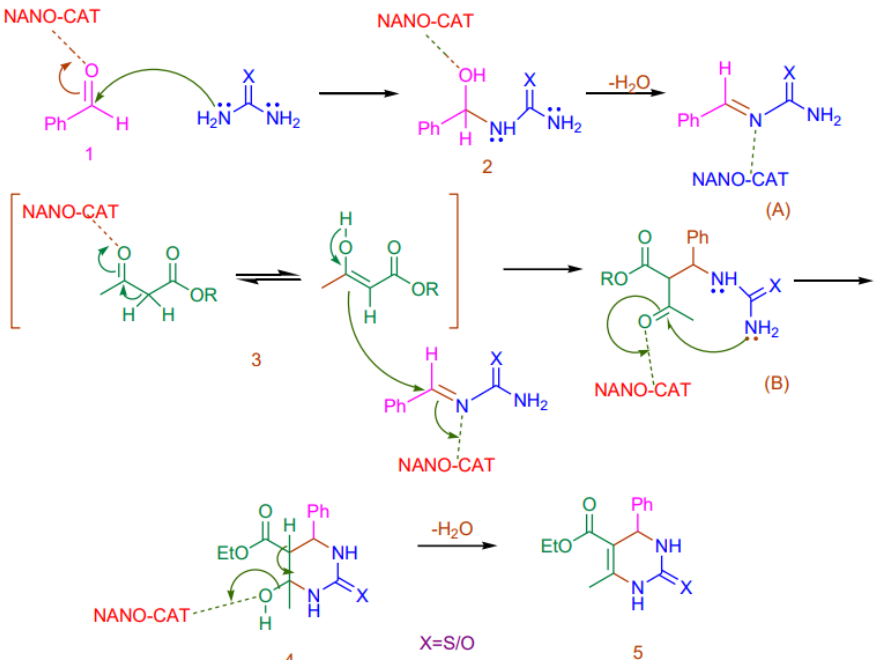

Figure 2. Proposed mechanism of synthesis of 3, 4-dihydropyrimidin-2(1H)-ones/thiones.

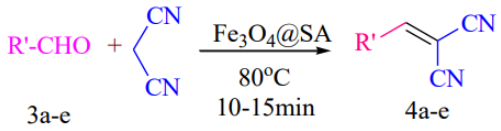

Scheme 3. Synthesis of benzylidenemalononitrile (4a-4e) by Fe_3O_4@SA catalyst at solvent-free condition.

4-dihydropyrimidin-2(1H)-ones/thiones. The first probable stage likely involves the rate-controlling nucleophilic addition of urea to an aldehyde activated by a catalyst, resulting in the formation of the N-alkylidene urea intermediate (A) through dehydration. The intermediate imine (A) was intercepted by the enolized acetoacetate, leading to the formation of intermediate (B). This intermediate then underwent consecutive cyclization and dehydration catalyzed by the reaction environment, ultimately yielding the anticipated dihydropyrimidinones/thiones 5.

To explore the catalytic activity and versatility of Fe_3O_4@SA magnetic nanocatalyst, it was tested for the synthesis of benzylidenemalononitrile. The synthesis of benzylidenemalononitrile using a nanocatalyst resulted in the formation of the corresponding condensation product (4a-4e) in 91-96% yield within 10-15 minutes of stirring (scheme 3) (Table 4, entry 1-5).

To assess the appropriateness of this synthetic approach, the Knoevenagel condensation of a model reaction was evaluated against other methods documented in the literature (Table 5, entry 1-8). This study offers benefits such as simplicity, similar reusability, eco-friendly and green conditions, a reasonable amount of catalyst, and brief reaction times.

3.1 Characterization of the Fe_3O_4@SA nanocatalyst

Various techniques were used to characterise the synthesized catalyst, such as FTIR, FE-SEM, TEM, SEM–EDS, XRD, TGA and VSM, etc.

Fourier-transform infrared spectroscopy (FTIR) is particularly effective for characterizing the functionalization and modification of magnetite nanoparticles. Infrared absorption spectra were obtained in the range from 3778 to 500 cm^{-1}. To authenticate the modification of the magnetite surface with salicylic acid and metal ions, nanocomposites were analyzed using FTIR spectra of magnetite, Fe_3O_4@SA, and salicylic acid. Fig. 3 shows the typical FTIR spectrum of (a) Fe_3O_4 nanoparticles (b_1)

Table 4. Synthesis of benzylidenemalononitrile (4a-4e) by Fe_3O_4@SA catalyst at solvent-free condition (Scheme 3).

Entry	Sr. No.	Reactant	Time (min)	Product	[b]Yield %	M.P.
1	**4a**	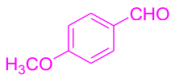	10	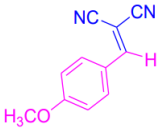	94	115 °C
2	**4b**	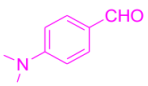	10	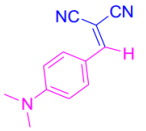	96	180 °C
3	**4c**	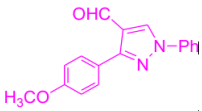	15	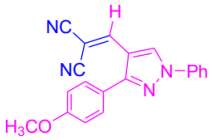	91	177-178 °C
4	**4d**	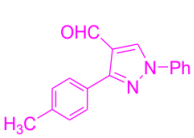	15	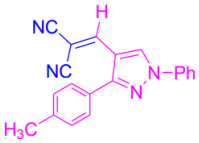	95	235-237 °C
5	**4e**	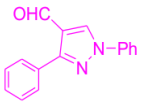	15	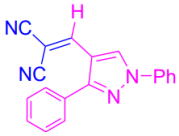	96	159-162 °C

Reaction condition: aromatic aldehyde (1 mmol), malononitirile (1 mmol), catalyst (0.050 g), reaction time 10-15 min, reaction temp 80 °C. [b] isolated yield.

Table 5. Catalytic activities of different catalysts for the synthesis of benzylidenemalononitrile.

Entry	Catalyst	Temp (°C)	Time (min)	Yield (%)	Solvent	Ref.
1	Fe_3O_4@APTMS@Zr-Sb-Ni-Zn	Reflux	25	93	Water	[61]
2	ZnO	RT	90	85	SF	[62]
3	Fe_3O_4-cysteamine hydrochloride	50	55	98	EtOH-H_2O	[63]
4	[Fe_3O_4@SiO_2@$(CH_2)_3$-caffein]OH	60	7	85	H_2O	[64]
5	$CaFe_2O_4$	Reflux	30	85	MeOH	[65]
6	Fe_3O_4@SiO_2@CuO-Fe_2O_3	Reflux	20	95	H_2O	[66]
7	CSC-Star-Glu-IL2	60	30	95	H_2O	[67]
8	Fe_3O_4@SA	80	10	94	SF	This work

The synthesis of benzylidenemalononitrile is achieved by Knoevenagel condensation of malononitrile, and 4-methoxy benzaldehyde (**3a**). The catalytic activity of certain heterogeneous solid acid catalysts is compared in solvent and solvent-free conditions.

Reused Fe_3O_4@Salicylic acid nanocomposite (b) Fresh Fe_3O_4@Salicylic acid nanocomposite and (c) Salicylic acid. The FT-IR spectrum of salicylic acid revealed asymmetric and symmetric vibrational peaks at wavenumbers 2980 cm^{-1} and 2850 cm^{-1}, respectively, which were attributed to C-H stretching presented in Fig. 3 (c). The presence of the C=O stretching band resulted in the acute peak at 1653 cm^{-1} (COO-). Notably, the peak at 3230 cm^{-1} was attributed to the -OH stretching frequency, a common feature in compounds with hydroxyl groups. The asymmetric and symmetric C-H stretching vibrations changed very little in the spectrum of salicylic acid-coated Fe_3O_4, as shown in Fig. 3(b). It is apparent that the IR spectra Fe_3O_4 & Fe_3O_4@SA nanoparticles show a sharp broad peak characteristic magnetite absorption for Fe-O stretching vibration, at 560 cm^{-1} are shown in Fig. 3.

It's noteworthy that the C=O stretching band of the carboxyl group, typically present at 1653 cm^{-1} in the pure salicylic acid spectrum, was absent in the nanocomposite spectrum. Two binding modes for surface carboxylate bonding have been proposed. However, only one peak at 1400 cm^{-1} corresponding to symmetric stretching was observed. Consequently, we conclude that salicylic acid adsorbs on the surface of Fe_3O_4 symmetrically through two oxygen atoms of the carboxylate group, indicating the linkage of salicylic acid to the Fe_3O_4 nanoparticle surface [68–71]. There was no notable change in the IR spectra between the fresh catalyst and the catalyst reused four times, indicating its stability Fig. 3(b_1).

Primarily, the size, structure, and morphology of Fe_3O_4@Salicylic acid nanocomposite were investigated by FESEM images (Fig. 4). A typical FESEM image of salicylic acid Fe_3O_4 nanocomposite is shown in Fig. 4. The morphology of the nanocomposite was observed through FESEM images. The images clearly indicate that these nanoparticles have appeared as spherical shape structures with average grain size of 10 to 25 nm are shown in Fig. 4. The round surface of MNP's is obvious, which provides the active surface area for adsorption of the reactant molecule. Transmission electron microscopy (TEM) examination was used to examine the shape and microstructure of the nanoscale particles. The TEM images presented in Fig. 5 demonstrate spherical Fe_3O_4@SA nano sized particles, with an average size ranging from 10 to 25 nm.

Furthermore, energy X-ray spectroscopy (FESEM–EDS) was used to ascertain the chemical composition of the Fe_3O_4@SA nanomaterial. Images from elemental mapping verified the existence of C, O, and Fe in the nanomaterial (Fig. 6). Energy dispersive X-ray spectra were used to compute the percentages of each element contained in the nanocatalyst, and the results were in good agreement with the catalyst composition that was suggested. An alternate name for the stoichiometric magnetite Fe_3O_4 is FeO•Fe_2O_3. As a result, it has salicylic acid and iron ions Fe^{2+} and Fe^{3+}

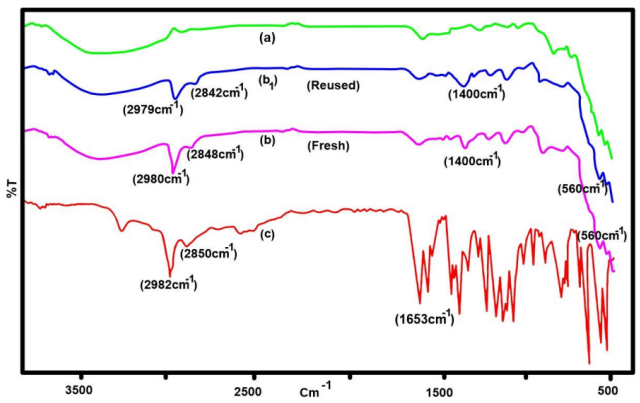

Figure 3. FT-IR spectra of (a) Fe_3O_4 nanoparticles (b_1) Reused Fe_3O_4@Salicylic acid nanocomposite (b) Fresh Fe_3O_4@Salicylic acid nanocomposite and (c) Salicylic acid.

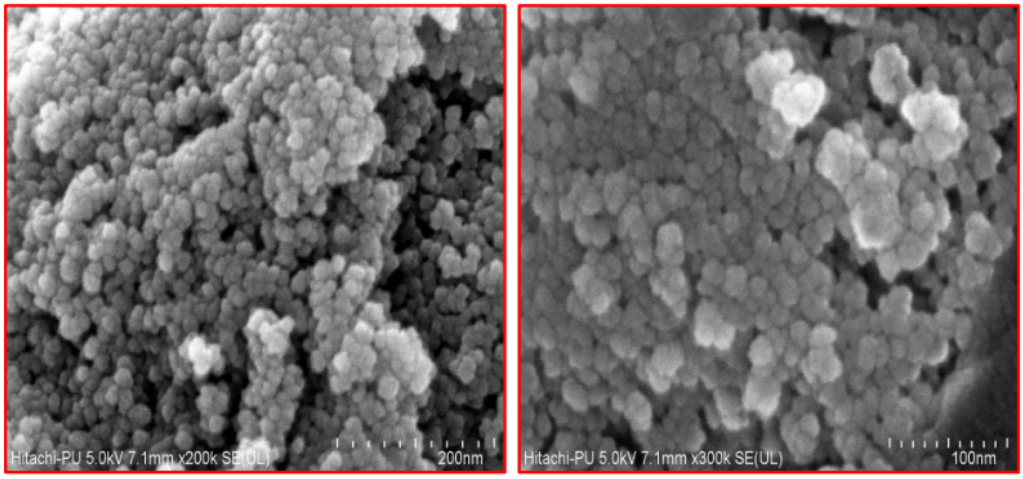

Figure 4. FE-SEM images of Fe_3O_4@SA nanocatalyst.

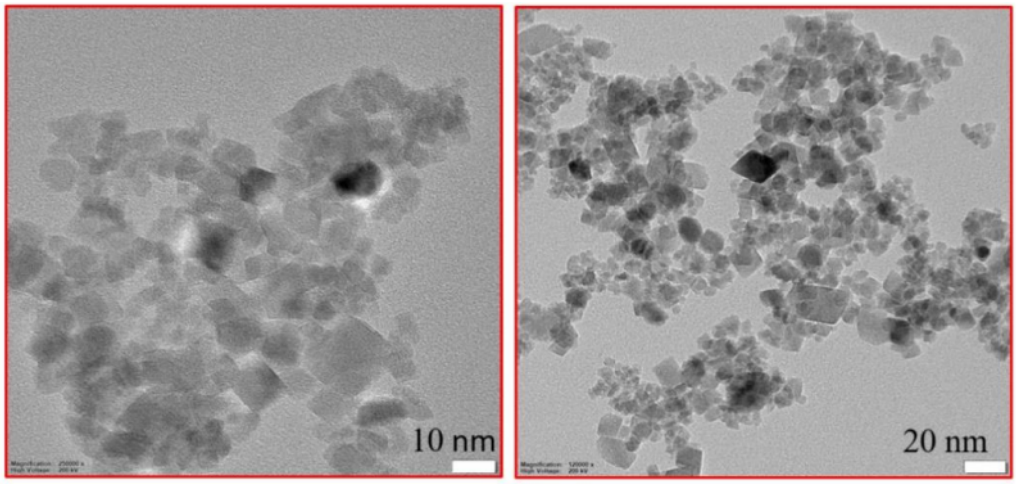

Figure 5. TEM images of Fe_3O_4@SA nanocatalyst sample.

in its structure. In the EDS spectra of Fe_3O_4@SA (Fig. 6), it is observed that the binding energies of C, O, Fe^{2+}, and Fe^{3+} are associated with the peaks that emerge at 0.27, 0.51, 0.70, and 6.39 keV, respectively (Fig. 6).

To investigate the crystal composition of the generated nanoparticles X-ray diffraction was performed. The X-ray diffraction (XRD) patterns of (X1) Fe_3O_4 and (X2) Fresh Fe_3O_4@SA are shown in Fig. 7. In the XRD spectra diffraction peaks with 2θ at 30.52°, 35.78°, 43.67°, 54.35°, 57.34°, 63.07° are observed, which indicate that the Fe_3O_4 particles have a crystalline structure (Fig. 7) . Curve X2, representing Fe_3O_4@SA, exhibits a similar XRD pattern to curve X1, indicating that the structure of Fe_3O_4 nanoparticles remains unchanged after the addition of the salicylic acid layer. The XRD patterns (X3) revealed no significant changes in the crystallographic structure of the catalyst after four reuse cycles, indicating the preservation of its crystalline phase.

The average crystallite size of the catalysts, determined using the Debye-Scherrer equation, was found to be 22.48 nm, which is consistent with the range observed in the TEM results of 10 to 25 nm.

Within the measurement temperature range, Fe_3O_4 exhibits no weight loss. This shows that within the studied temper-

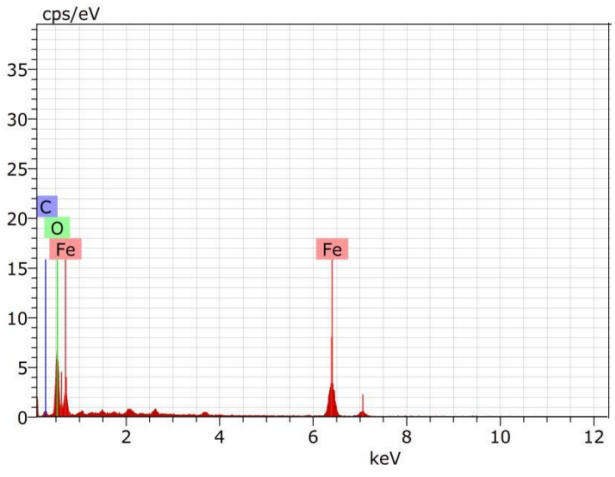

Element	Series	unn. C [Wt. %]	norm. C [Wt. %]	Atom. C [At. %]	Error (3 Sigma) [Wt. %]
Iron	K-series	54.66	66.76	35.85	5.36
Oxygen	K-series	24.78	30.27	56.73	10.86
Carbon	K-series	2.44	2.97	7.42	4.15
Total:		81.88	100.00	100.00	

Figure 6. EDS profile of Fe_3O_4@SA nanocatalyst sample.

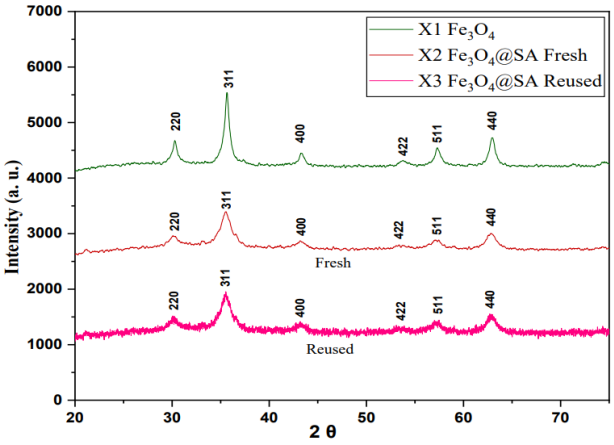

Figure 7. XRD of Fe_3O_4 and nanocatalyst Fe_3O_4@SA.

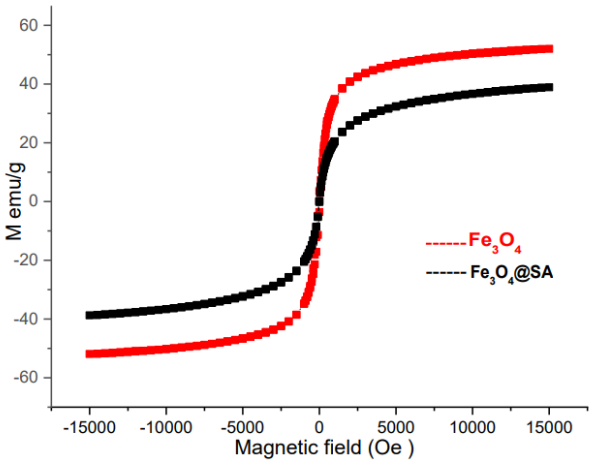

Figure 9. VSM of Fe_3O_4 and nanocatalyst Fe_3O_4@SA.

ature range, Fe_3O_4 is stable and does not significantly decompose or change weight. Between ambient temperature and 400°C, the weight of the nanocomposite is seen to decrease by approximately ∼2.5 weight percent. This weight loss is attributed to the evaporation of both physisorbed and loosely coordinated water from the interlayer. In the 400-1000°C temperature range, a secondary weight loss of ∼8 wt% is ascribed to salicylic acid decomposition (as shown in Fig. 8).

VSM analysis was performed to verify the magnetic property of the produced nanocatalyst. The Fe_3O_4 and Fe_3O_4@SA magnetization curves are displayed in Fig. 9. The absence of hysteresis in the graph indicates that the sample is superparamagnetic. Fe_3O_4@SA (MNC) Magnetic nanocomposites saturation magnetic moment (Ms) was measured and found to be 51.90 emu/g (Fig. 9). The high of this value indicates that Fe oxidation is either low or absent. It was noticed that the saturation magnetization (Ms) of uncoated Fe_3O_4 decreases upon being coated with salicylic acid.

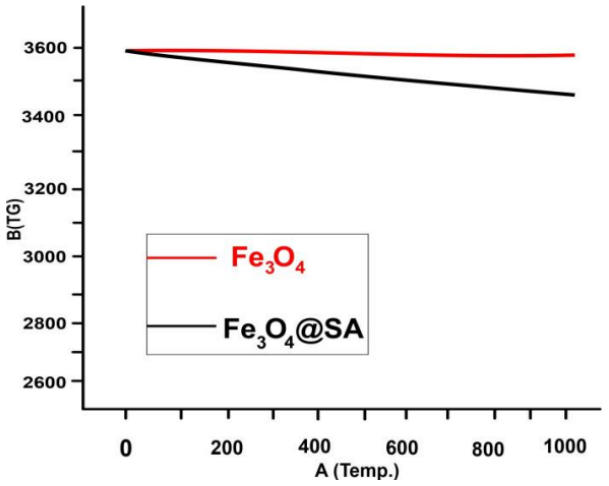

Figure 8. TGA of Fe_3O_4 and nanocatalyst Fe_3O_4@SA.

4. Conclusion

In summary, we successfully synthesized and characterized salicylic acid supported on crystalline Fe_3O_4 using various techniques, including infrared spectroscopy, powder X-ray diffraction, field emission scanning electron microscopy (FESEM), transmission electron microscopy (TEM), FESEM-energy-dispersive X-ray spectroscopy, thermogravimetric analysis (TGA), and vibrating sample magnetometry (VSM). This novel nanocatalyst proved to be an effective heterogeneous catalyst for synthesizing 3, 4-dihydropyrimidin-2(1H)-ones and benzylidenemalononitrile in a solvent-free environment at 80°C. The Fe_3O_4@SA nanocatalyst retained its catalytic performance over multiple uses without significant activity loss. Thus, the Fe_3O_4@SA nanocatalyst presents itself as a strong alternative to conventional solid catalysts for Biginelli and Knoevenagel condensation reactions. Its beneficial properties, such as non-toxicity, ease of separation, and recyclability, make it a highly attractive option for chemical industry applications.

Acknowledgments

The authors are thankful to the Director of SAIF, Punjab University, Chandigarh, Punjab, India, and Labzone Services, Powai, Mumbai, for the spectral analysis. The authors would like to acknowledge to Dr. Babasaheb Ambedkar, Marathwada University, Aurangabad-431004 (M.S.), India, for their support and for providing the necessary laboratory facilities and constant encouragement.

Authors Contributions

Authors have equal contribution role in preparing the paper.

Availability of Data and Materials

The data that support the findings of this study are available from the corresponding author upon reasonable request.

Conflict of Interests
The authors declare that they have no known competing financial interests or personal relationships that could have appeared to influence the work reported in this paper.

References

[1] A. Marandi, N. Koukabi, and A Physicochem. *Eng. Asp.*, **621**(2021):126597, . DOI: https://doi.org/10.1016/j.colsurfa.2021.126597.

[2] A. Marandi, N. Koukabi, and M. A. Zolfigol. *Res. Chem. Intermed.*, **47**(2021)(8):3145–63, . DOI: https://doi.org/10.1007/s11164-021-04457-z.

[3] T. Marzieh, K. Nadiya, and A. Ozra. *Heterocycl. Comm.*, **28**(2022):1–10. DOI: https://doi.org/10.1515/hc-2022-0003.

[4] a) A. Maleki and V. Eskandarpour. *J. Iran. Chem. Soc.*, **16**(2019)(7):1459–72. DOI: https://doi.org/10.1007/s13738-019-01610-9.

[5] A. Maleki, Z. Hajizadeh, and R. Firouzi-Haji. *Microporous Mesoporous Mater.*, **259**(2018):46–53, . DOI: https://doi.org/10.1016/j.micromeso.2017.09.034.

[6] A. Marandi, E. Nasiri, N. Koukabi, and F. Seidi. *Int. J. Biol. Macromol*, **190**(2021):61–71, . DOI: https://doi.org/10.1016/j.ijbiomac.2021.08.085.

[7] R.B.N. Baig and R.S. Varma. *Chem. Commun.*, **49**(2013)(8):752–70. DOI: https://doi.org/10.1039/C2CC35663E.

[8] K.X. Nguyen, P.H. Pham, A.C.D. Nguyen, C.T. Nguyen, T.T. Nguyen, and P.D. Tran. *J. Ind. Eng. Chem.*, **92**(2020):96–100. DOI: https://doi.org/10.1016/j.jiec.2020.08.027.

[9] M. Kaur, B. D. Mayank, G. Singh, N. Kaur, and N. Singh. *Polym. Chem.*, **12**(2021)(8):1165–75. DOI: https://doi.org/10.1039/D0PY01769H.

[10] Z. Zhao, H. Dai, and L. Shi. *Chem. Pap.*, **75**(2021)(2):583–90. DOI: https://doi.org/10.1007/s11696-020-01327-7.

[11] D. K. Mondal, G. Phukan, N. Paul, and J. P. Borah. *J. Magn. Magn. Mater*, **528**(2021):167809, . DOI: https://doi.org/10.1016/j.jmmm.2021.167809.

[12] M. Xing, J. Mohapatra, J. Beatty, J. Elkins, N.K. Pandey, and A. Chalise. *J. Alloy Compd.*, **871**(2021):159475. DOI: https://doi.org/10.1016/j.jallcom.2021.159475.

[13] L. Wang, X. Huang, C. Wang, X. Tian, X. Chang, and Y. Ren. *Food Chem.*, **342**(2020):128343. DOI: https://doi.org/10.1016/j.foodchem.2020.128343.

[14] Y.Yin, Y. Li, S. Wang, Z. Dong, C. Liang, J. Sun, C. Wang, R. Chai, W. Fei, J.Zhang, M. Qi, L.Feng, and Q. Zhang. *J. Nanobiotechnology*, **19**(2021)(1):1–13. DOI: https://doi.org/10.1186/s12951-021-00823-6.

[15] B. C. Van, D. Punihaole, A.R. Keith, A. J. Schmitz, J. Tolar, and R. R. Frontiera. *Proc. Natl. Acad. Sci.*, **117**(2020)(52):32919–28. DOI: https://doi.org/10.1073/pnas.2016860117.

[16] J. Mondal, T. Sen, and A. Bhaumik. *Dalt. Trans.*, **41**(2012)(20):6173–81, . DOI: https://doi.org/10.1039/c2dt30106g.

[17] N. Koukabi, E. Kolvari, A. Khazaei, M.A. Zolfigol, B. ShirmardiShaghasemi, and H.R. Khavasi. *Chem. Commun.*, **47**(2011):9230–2. DOI: https://doi.org/10.1039/c1cc12693h.

[18] C.W. Lim and I. S. Lee. *Nano Today*, **5**(2010)(5):412–34. DOI: https://doi.org/10.1016/j.nantod.2010.08.008.

[19] K. Xu, L. Jiao, C. Wang, Y. Bu, Y. Tang, and L. Qiu. *J. Env. Sci.*, **111**(2022):93–103. DOI: https://doi.org/10.1016/j.jes.2021.03.020.

[20] A. Maleki, A.A. Jafari, and S. Yousefi. *J. Iran. Chem. Soc.*, **14**(2017)(8):1801–13, . DOI: https://doi.org/10.1007/s13738-017-1120-2.

[21] N. E. Masoud, S. J. Hoseini, and M. Fatemeh. *Chin. J. Catal.*, **32**(2011):1484–1489. DOI: https://doi.org/10.1016/S1872-2067(10)60263-X.

[22] E. Mohsen, J. Jaber, and N. D. Fatemeh. *RSC Adv*, **5**(2015):308–310. DOI: https://doi.org/10.1039/c4ra09929j.

[23] K. Mitlesh, J. Yachana, Y. Priya, and L. Harshita. *Catal. Lett.*, **149**(2019):2180–2194. DOI: https://doi.org/10.1007/s10562-019-02794-8.

[24] F. Moradi, M. Abdoli-Senejani, and M. Ramezani. *Curr. Org. Syn.*, **17**(2019)(1):46–54. DOI: https://doi.org/10.2174/1570179416666191118110316.

[25] J. Safari and Z. Zarnegar. *RSC. Adv*, **39**(2013):17962–17967. URL 10.1039/C3RA43014F.

[26] B. Dam, A. K. Pal, and A. Gupta. *Synth. Commun.*, **46**(2016):275–286. DOI: https://doi.org/10.1080/00397911.2015.1135955.

[27] T. F. Shaghayeghi, A. Maghsoodi, and F. S. Toosi. *Synth. React. Inorganic, Met. Nano-Metal Chem.*, **46**(2016):168–170. DOI: https://doi.org/10.1080/15533174.2014.900802.

[28] F. Zamani, S. M. Hosseini, and S. Kianpour. *Solid State Sci.*, **26**(2013):139–143. DOI: https://doi.org/10.1016/jsolidstatesciences.2013.10.007.

[29] F. Zamani and E. Izadi. *Catal. Commun.*, **42**(2013):104–108. DOI: https://doi.org/10.1016/J.CATCOM.2013.08.006.

[30] R. Tayebee, M. Fattahi Abdizadeh, N. Erfaninia, A. Amiri, M. Baghayeri, R. M. Kakhki, B. Maleki, and E. Esmaili. *Appl. Organomet. Chem.*, **33**(2019)(8):e4959. DOI: https://doi.org/10.1002/aoc.4959.

[31] F. Krauskopf, K. N. Truong, K. Rissanen, and C. Bolm. *Org. Lett.*, **23**(2021)(7):2699–2703. DOI: https://doi.org/10.1021/acs.orglett.1c00596.

[32] L. G. D. Nascimento, I. M. Dias, G. B. M. de Souza, I. DanciniPontes, N. R. C. Fernandes, P. S. de Souza, G. R. de Oliveira, and C. G. Alonso. *J. Org. Chem.*, **85**(2020)(17):11170–11180. DOI: https://doi.org/10.1021/acs.joc.0c01167.

[33] N. M. Chavhan, S. D. Bhakare, R. C. Muthe, S.Y. Hande, A. S. Gandule, D. N. Gaikwad, and D. M. Suryawanshi. *Lett. in Org. Chem.*, **19**(2022):1–3. DOI: https://doi.org/10.2174/1570178619666220113114613.

[34] C. O. Kappe. *Tetrahedron*, **49**(1993)(32):6937–6963, . DOI: https://doi.org/10.1016/S0040-4020(01)87971-0.

[35] C. O. Kappe and S. Alexander. *Org. Reactions*, **63**(2004):1–116. DOI: https://doi.org/10.1002/0471264180.or063.01.

[36] R. K. Singh, K. Sahore, R. Rana, S. Kumar, and D.N. Prasad. *Iran. J. Catal.*, **6**(2016)(4):389–408.

[37] J. P. Wan and Y. Pan. *Mini-Reviews in Med. Chem.*, **12**(2012):337–349. DOI: https://doi.org/10.2174/138955712799829267.

[38] J. P. Wan, Y. Lin, and Y. Liu. *Cur. Org. Chem.*, **18**(2014)(6):687–699. DOI: https://doi.org/10.2174/1385272818061404152358 55.

[39] A. Suresh and J. S. Sandhu. *ARKIVOC. (i)*, (2012):66–133. DOI: https://doi.org/10.3998/ark.5550190.0013.103.

[40] M. A. S. Abdullah and A. N. A. Abdul-salam. *Synth. Commun.*, **19**(2018):1–20. DOI: https://doi.org/10.1080/00397911.2018.1536789.

[41] C. O. Kappe. *Eur. J. Med. Chem.*, **35**(2000): 1043–1052, . DOI: https://doi.org/10.1016/S0223-5234(00)01189-2.

[42] G. C. Rovnyak, K. S. Atwal, A. Hedberg, S. D. Kimball, S. Moreland, J. Z. Gougoutas, B. C. O'Reilly, J. Schwartz, and M. F. Malley. *J. Med. Chem.*, **35**(1992):3254–3263. DOI: https://doi.org/10.1021/jm00095a023.

[43] D. Nagarathnam, S. W. Miao, B. Lagu, G. Chiu, J. Fang, T. G. Murali Dhar, J. Zhang, S. Tyagarajan, M. R. Marzabadi, F. Zhang, W. C. Wong, W. Sun, D. Tian, J. M. Wetzel, C. Forray, R. S. Chang, T. P. Broten, R. W. Ransom, T. W. Schorn, T. B. Chen, S. O'Malley, P. Kling, K. Schneck, R. Bendesky, and C. M. Harrell. *J. Med. Chem.*, **42**(1999):4764–4777. DOI: https://doi.org/10.1021/jm990200p.

[44] J. C. Barrow, P. G. Nantermet, H. G. Selnick, K. L. Glass, K. E. Rittle, K. F. Gilbert, T. G. Steele, C. F. Homnick, R. M. Freidinger, and R. W. Ransom. *J. Med. Chem.*, **43**(2000):2703–2718. DOI: https://doi.org/10.1021/jm990200p.

[45] D. Russowsky, R. F. S. Canto, S. A. A. Sanches, M. G. M D'Oca, A. de Fatima, R. A. Pilli, L. K. Kohn, M. A. Antonio, and J. E. de Carvalho. *Bioorg. Chem.*, **34**(2006):173–182. DOI: https://doi.org/10.1016/j.bioorg.2006.04.003.

[46] M. M. Heravi and V. Zadsirjan. *Curr. Org. Chem.*, **24**(2020)(12):1331–1366. DOI: https://doi.org/10.2174/1385272824999200616111228.

[47] M. B. Gawande, D. M. Nagrik, and M. D. Ambhore. *Lett. in Org. Chem.*, **9**(2012)(1):12–18. DOI: https://doi.org/10.2174/157017812799303980.

[48] S. S. Panda, P. Khanna, and L. Khanna. *Curr. Org. Chem.*, **16**(2012)(4):507–520. DOI: https://doi.org/10.2174/157017812799303980.

[49] N. Zengin, H. Burhan, A. Şavk, H. Göksu, and F. Şen. *Sci. Rep.*, **10**(2020):12758. DOI: https://doi.org/10.1038/s41598-020-69764-8.

[50] Q. Hu, X.-L. Shi, Y. Chen, X. Han, P. Duan, and W. Zhang. *J. Ind. Eng. Chem.*, **54**(2017):75–81. DOI: https://doi.org/10.1016/J.JIEC.2017.05.020.

[51] S. A. Khan, A. M. Asiri, R. M. A. Rahman, S. A. Elroby, F. M. S. Aqlan, M.Y. Wani, and K. Sharma. *J. Heterocycl. Chem.*, **54**(2017):3099–3107. DOI: https://doi.org/10.1002/JHET.2923.

[52] O. M. Abo-El-Enien F. A. Agizah A. S. Fouda, Y. A. El-Ewady. *Anti-Corr. Methods Mater*, **55**(2008):317–323. DOI: https://doi.org/10.1108/00035590810913105.

[53] N.Zengin, H. Burhan, A.Şavk, H. Göksu, and F. Şen. *Sci. Rep.*, **10**(2020):12758. DOI: https://doi.org/10.1038/s41598-020-69764-8.

[54] J. B. M. De Resende Filho, G. P. Pires, J. M. G. de Oliveira Ferreira, E. E. S. Teotonio, and J. A. Vale. *Catal. Letters.*, **147**(2017):167–180. DOI: https://doi.org/10.1007/s10562-016-1916-1.

[55] M. B. Gawande and R. V. Jayaram. *Catal. Commu.*, **7**(2006):931–935. DOI: https://doi.org/10.1016/j.catcom.2006.03.008.

[56] N. Yao, J. Tan, Y. Liu, and Y. L. Hu. *Syn. lett.*, **30**(2019)(06):699–702. DOI: https://doi.org/10.1055/s-0037-1612076.

[57] R. Maleki, R. Kolvari, E. Salehi, and M. Koukabi. *Appl. Organomet. Chem.*, **31**(2017)(11):e3795, . DOI: https://doi.org/10.1002/aoc.3795.

[58] B. Maleki, F. Taheri, R. Tayebee, and F. Adibian. *Org. Prep. Proced. Int.*, **53**(2021)(3):284–290, . DOI: https://doi.org/10.1080/00304948.2021.1875799.

[59] F. Hajizadeh, B. Maleki, F.M. Zonoz, and A. Amiri. *J. Iran. Chem. Soc.*, **18**(2021):793–804. DOI: https://doi.org/10.1007/s13738-020-02071-1.

[60] D. N. Gaikwad, S. T. Gaikwad, R. K. Manjul, A. S. Rajbhoj, and D. M. Suryavanshi. *Lett. in Org. Chem.*, **28**(2024)(4). DOI: https://doi.org/10.2174/0113852728284846240124052127.

[61] M. Gilanizadeh and B. Zeynizadeh. *Canadian Journal of Chemistry*, **99**(2021)(6):531–539, . DOI: https://doi.org/10.1139/cjc-2020-0421.

[62] M. Basude, P. Sunkara, and V. S. Puppala. *J. Chem. Pharm. Res.*, **5**(2013):46–50.

[63] R. Maleki, E. Kolvari, M. Salehi, and N. Koukabi. *Appl. Organomet. Chem.*, **31**(2017)(11):e3795, . DOI: https://doi.org/10.1002/aoc.3795.

[64] M. Javdannezhad, M. Gorjizadeh, M. H. Sayahi, and S. Sayyahi. *J. Nanoanalysis*, **5**(2018)(4):287–293. DOI: https://doi.org/10.22034/jna.2018.545583.

[65] P. Pippal and P. P. Singh. *Orient. J. Chem.*, **33**(2017)(4):1736–1743. DOI: https://doi.org/10.13005/ojc/330418.

[66] M. Gilanizadeh and B. Zeynizadeh. *Res. Chem. Intermed.*, **44**(2018):6053–6070, . DOI: https://doi.org/10.1007/s11164-018-3475-0.

[67] P. Gupta, M. Kour, S. Paul, and J. H. Clark. *RSC Adv.*, **4**(2014)(15):7461–7470. DOI: https://doi.org/10.1039/c3ra45229h.

[68] S. Xuan, L. Hao, W. Jiang, X. Gong, and Z. Chen Y. Hu. *J. Magn. Magn. Mater.*, **308**(2007):210–213. DOI: https://doi.org/10.1016/j.jmmm.2006.05.017.

[69] L. Zhang, R. He, and H. Gu. *Appl. Surf. Sci.*, **253**(2006):2611–2617. DOI: https://doi.org/10.1016/J.APSUSC.2006.05.023.

[70] G. Kataby, M. Cojocaru, R. Prozorov, and A. Gedanken. *Langmuir*, **15**(1999):1703–1708. DOI: https://doi.org/10.1021/LA981001W.

[71] B. Unal, Z. Durmus, H. Kavas, A. Baykal, and M.S. Toprak. *Materials Chemistry and Physics*, **123**(2010):184–190. DOI: https://doi.org/10.1016/j.matchemphys.2010.03.080.